Switchable Truncations Between the 1st- and 2nd-Order DZT-CFS-UPMLs for Relevant FDTD Problems

Naixing Feng, *Member, IEEE,* Jingang Wang, Jinfeng Zhu, *Senior Member, IEEE,* Zhongzhu Liang, Guo Ping Wang, and William T. Joines, *Life Fellow, IEEE*

***Abstract*— Adopting the direct *Z*-transform (DZT) method due to its higher accuracy instead of the approximate *Z*-transform (AZT) methods and efficient and switchable truncations between the 1st- and 2nd-order uniaxial perfectly matched layers (UPMLs) with the complex-frequency-shifted (CFS) scheme are shown to terminate the relevant finite-difference time-domain (FDTD) regions. The proposed DZT-CFS-UPML formulations can possess the switchable function in terms of relevant FDTD problems so that the optimal performance can be obtained with the tradeoff among memory requirement, CPU time, and absorption accuracy. For the FDTD problem with the strong evanescent and weak low-frequency propagating waves, the proposed DZT-CFS-UPML formulations can be switched to the 1st-order PML truncation, and for the other cases with both low-frequency propagating and strong evanescent waves, the 2nd-order PML is the best choice. Two numerical simulations have been carried out to illustrate the validity and flexibility of the proposed approach.**

***Index Terms*— Complex-frequency-shifted uniaxial perfectly matched layer (CFS-UPML), direct *Z*-transform (DZT) method, finite-difference time-domain (FDTD), switchable function.**

I. Introduction

BY USING unsplitted-field implementations, the stretched coordinate perfectly matched layer (SC-PML) [1]–[9] and the uniaxial PML (UPML) [10], [11] have been developed to consume less CPU time and memory to great extent, since the splitted-field-based PML method was first proposed in 1994 [12] to terminate the regular finite-difference time-domain (FDTD) computational region [13]. Generally, PML expressions are usually defined and written in the frequency domain. So far, several techniques have been successfully utilized to discretize PML formulations by adopting the auxiliary differential equations (ADEs) techniques [1], [2] or the *Z*-transform methods [3]–[8]. Why are *Z*-transform methods quite popular and prevailing for the discretization in FDTD implementations? The main reason is that the convolution in the time domain is just a kind of multiplication in the *Z*-domain; however, complicated convolutional computations will be never circumvented if the transformation happens from the frequency domain to the time domain [14], [15].

In addition, as described in [14] and [15], two classes of the *Z*-transform techniques can be chosen. The first one is the direct *Z*-transform (DZT) method, which is the most accurate due to the fact that it can convert from terms in the frequency domain to those in the *Z* domain via looking them up in a table; and the another one is the matched *Z*-transform (MZT) and bilinear *Z*-transform (BZT) methods that are always easier due to using direct substitution.

To the best of our knowledge, however, the regular SC and UPMLs have the same drawback as the regular PML, leading to their low efficiencies in absorbing evanescent waves. To conquer this problem, authors proposed the complex-frequency-shifted PML (CFS-PML) formulations, resulting in highly effective absorption for strong evanescent waves and reducing the late-time reflections [16]–[21].

Recently, to pursuing higher accuracies, several higher order PML implementations have been presented for truncating the FDTD domain [22]–[27]. Besides, among these higher order PMLs, the 2nd-order PML has been validated and proved to be an optimal choice [28].

As is well known to all, for the problem with the strong evanescent and weak low-frequency propagating waves, the 1st-order PML is the optimal choice, so that more CPU time and memory requirement can be saved; and for the other cases with both the low-frequency propagating and strong evanescent waves, the 2nd-order PML is the best choice for higher accuracies, although more CPU time and memory are required.

To achieve both higher accuracy in absorption performance and lower consumption in CPU time and memory,

Manuscript received September 19, 2018; revised June 6, 2019; accepted July 6, 2019. Date of publication July 26, 2019; date of current version January 3, 2020. This work was supported in part by NSFC under Grant 11734012, Grant 11574218, Grant 6173000222, Grant U1830116, and Grant 61376122, in part by the Youth Innovation Promotion Association Chinese Academy of Sciences (CAS) under Grant 2014193, and in part by the State Key Laboratory of Applied Optics Independent Fund. *(Corresponding authors: Jinfeng Zhu; Guo Ping Wang.)*

N. Feng and G. Wang are with the Institute of Microscale Optoelectronics, Shenzhen University, Shenzhen 518060, China (e-mail: gpwang@szu.edu.cn).

J. Wang is with the College of Science, Liaoning Shihua University, Fushun 113001, China.

J. Zhu is with the School of Electronic Science and Engineering, Xiamen University, Xiamen 361005, China, and also with the Shenzhen Research Institute of Xiamen University, Shenzhen 518057, China (e-mail: nanoantenna@hotmail.com).

Z. Liang is with the State Key Laboratory of Applied Optics, Changchun Institute of Optics, Fine Mechanics and Physics, Chinese Academy of Sciences, Changchun 130033, China.

W. T. Joines is with the Department of Electrical and Computer Engineering, Duke University, Durham, NC 27708 USA.

Color versions of one or more of the figures in this article are available online at http://ieeexplore.ieee.org.

Digital Object Identifier 10.1109/TAP.2019.2930118

the DZT-based FDTD implementation adopting SC-PML formulations with the CFS scheme is shown in [29]. Depending on this successful work in [29], therefore, switchable truncations between the 1st- and 2nd-order DZT-based CFS-UPMLs are studied in this work to enrich choices of DZT-based UPML implementations and make themselves easily mastered and used by beginners. In this paper, efficient FDTD implementations of 1st- and 2nd-order DZT-based CFS-UPMLs are proposed to truncate relevant FDTD cases, and this method is here referred as the DZT-CFS-UPML.

This paper is properly organized as follows. In Section II, the proposed DZT-based CFS-UPMLs are developed. Two numerical examples are presented in Section III. Section IV concludes this paper.

II. Formulations

In 3-D UPML regions, the modified Maxwell's curl equations in the frequency domain can be described as follows:

$$j\omega\varepsilon_0\varepsilon_r(\omega)\Lambda(\omega)E(\omega) = \nabla \times H(\omega) \tag{1}$$

$$j\omega\mu_0\mu_r(\omega)\Lambda(\omega)H(\omega) = -\nabla \times E(\omega) \tag{2}$$

where both ε_r and μ_r are the relative permittivity and permeability in the FDTD domain, respectively, and $\Lambda(\omega)$ is a diagonal tensor defined as follows:

$$\Lambda(\omega) = \text{diag}\left\{\frac{S_yS_z}{S_x}, \frac{S_xS_z}{S_y}, \frac{S_xS_y}{S_z}\right\} \tag{3}$$

where $S_\eta, (\eta = x, y, z)$ are complex stretched coordinate variables defined as follows:

$$S_\eta = \prod_{i=1}^{2} S_{i\eta} = \prod_{i=1}^{2}\left(\kappa_{i\eta} + \frac{\sigma_{i\eta}}{\alpha_{i\eta} + j\omega\varepsilon_0}\right) \tag{4}$$

where $\kappa_{i\eta}$ is real and ≥ 1, and $\sigma_{i\eta}$ and $\alpha_{i\eta}$ are assumed to be the positive real. It should be noted that we here adopt the one- and two-pole CFS-UPMLs. To let the CFS-UPML be absolutely independent of the material attributes of the FDTD computational domains, both (1) and (2) can be rewritten in terms of the electric flux density D and the magnetic flux density B, respectively, [23], [24]

$$j\omega\Lambda(\omega)D(\omega) = \nabla \times H(\omega) \tag{5}$$

$$j\omega\Lambda(\omega)B(\omega) = -\nabla \times E(\omega). \tag{6}$$

Therefore, this kind of UPML can be used for truncating any media, such as dispersive, lossy, inhomogeneous, anisotropic, or nonlinear with no any changes. This method can be obtained in [27] to get H from B [and E from D].

To simplify the left-hand side of expressions in (5) and (6), two auxiliary variables F and G in the frequency domain can be used to denote the right-hand side of (5) and (6), we have

$$F(\omega) = j\omega\Lambda(\omega)D(\omega) \tag{7}$$

$$G(\omega) = j\omega\Lambda(\omega)B(\omega). \tag{8}$$

Now, let us take the discretization of the x component of (7) in the corner of UPML regions, which can be obtained as follows:

$$F_x(\omega) = j\omega\Lambda_x(\omega)D_x(\omega). \tag{9}$$

Rearranging (9), we obtain

$$D_x(\omega) = j\omega^{-1}\left(\frac{S_yS_z}{S_x}\right)^{-1} F_x(\omega). \tag{10}$$

Here, the 1st-order CFS-UPML is considered in (10).

Multiplying $(j\omega^{-1}/j\omega^{-1})$ in the right-hand side of (10), we have

$$D_x(\omega) = \left(\frac{j\omega S_y \cdot j\omega S_z}{j\omega S_x}\right)^{-1} F_x(\omega). \tag{11}$$

Let us assume $J_\eta(\omega) = j\omega S_\eta(\omega)$,$(\eta = x, y, \text{or}z)$, we have

$$J_\eta = \frac{j\omega(\kappa_\eta\alpha_\eta + \sigma_\eta) + (j\omega)^2\kappa_\eta\varepsilon_0}{j\omega\varepsilon_0 + \alpha_\eta} = \frac{j\omega\kappa_\eta(j\omega + A_{1\eta})}{j\omega + A_{2\eta}}. \tag{12}$$

Tidying up (12), and we have

$$J_\eta^{-1} = \frac{A_{3\eta}}{j\omega + A_{1\eta}} + \frac{A_{4\eta}}{j\omega} \tag{13}$$

where

$$A_{1\eta} = \frac{\alpha_\eta}{\varepsilon_0} + \frac{\sigma_\eta}{\kappa_\eta\varepsilon_0}, \quad A_{2\eta} = \frac{\alpha_\eta}{\varepsilon_0},$$
$$A_{3\eta} = \frac{1}{\kappa_\eta}\left(1 - \frac{A_{2\eta}}{A_{1\eta}}\right), \quad A_{4\eta} = \frac{A_{2\eta}}{\kappa_\eta A_{1\eta}}.$$

Rearranging (13) with $\varphi_\eta = J_\eta^{-1}$,$(\eta = x, y, \text{or}z)$ below

$$D_x(\omega) = \frac{\varphi_y\varphi_z}{\varphi_x}F_x(\omega). \tag{14}$$

Next, introducing two auxiliary variables, ϕ_x, δ_x, we achieve

$$D_x(\omega) = \varphi_z(\omega)\phi_x(\omega) \tag{15}$$

$$\phi_x(\omega) = \varphi_y(\omega)\delta_x(\omega) \tag{16}$$

$$\delta_x(\omega) = (1/\varphi_x(\omega))F_x(\omega). \tag{17}$$

And then, we here adopt the DZT method and reach new DZT-based equations, which can be discretized as follows:

$$P_x^{n+1} = \frac{(A_{3x} + A_{4x}e^{-A_{1x}\Delta t})}{(A_{3x} + A_{4x})}P_x^n + F_x^{n+1} - F_x^n \tag{18}$$

$$\delta_x^{n+1} = P_x^{n+1} - e^{-A_{1x}\Delta t}P_x^n \tag{19}$$

$$\hat{\delta}_x^{n+1} = \hat{\delta}_x^n + A_{4y}\Delta t\delta_x^{n+1} \tag{20}$$

$$\phi_x^{n+1} = e^{-A_{1y}\Delta t}\phi_x^n + \hat{\delta}_x^{n+1} - e^{-A_{1y}\Delta t}\hat{\delta}_x^n + A_{3y}\Delta t\delta_x^{n+1} \tag{21}$$

$$\hat{D}_x^{n+1} = \hat{D}_x^n + A_{4z}\Delta t\phi_x^{n+1} \tag{22}$$

$$D_x^{n+1} = e^{-A_{1z}\Delta t}D_x^n + \hat{D}_x^{n+1} - e^{-A_{1z}\Delta t}\hat{D}_x^n + A_{3z}\Delta t\phi_x^{n+1} \tag{23}$$

where $P_x, \hat{\delta}_x, \hat{D}_x$ are introduced as auxiliary variables in (18)–(23).

The simulation pseudo-code of (18)–(23) is as follows:
1st step:

$$\text{temp\_}Fx = F_x^n, \quad \text{temp\_}\delta x = \delta_x^n$$
$$\text{temp\_}Px = P_x^n, \quad \text{temp\_}D_x^n = D_x^n$$
$$\text{temp\_}\phi x = \phi_x^n, \quad \text{temp\_}\hat{D}_x^n = \hat{D}_x^n, \quad \text{temp\_}\hat{\delta}_x^n = \hat{\delta}_x^n.$$

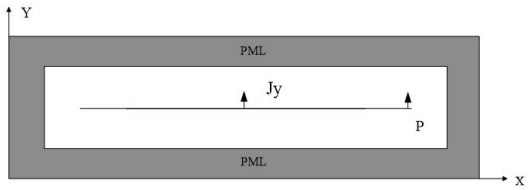

Fig. 1. FDTD grid geometry in this simulation.

2nd step:

$$P_x^{n+1} = \frac{(A_{3x} + A_{4x}e^{-A_{1x}\Delta t})}{(A_{3x} + A_{4x})}\text{temp\_}Px + F_x^{n+1} - \text{temp\_}Fx.$$

3rd step:

$$\delta_x^{n+1} = P_x^{n+1} - e^{-A_{1x}\Delta t}\text{temp\_}Px.$$

4th step:

$$\hat{\delta}_x^{n+1} = \text{temp\_}\hat{\delta}_x^n + A_{4y}\Delta t\delta_x^{n+1}.$$

5th step:

$$\phi_x^{n+1} = e^{-A_{1y}\Delta t}\text{temp\_}\phi x + \hat{\delta}_x^{n+1} - e^{-A_{1y}\Delta t}\text{temp\_}\hat{\delta}_x^n + A_{3y}\Delta t\delta_x^{n+1}.$$

6th step:

$$\hat{D}_x^{n+1} = \text{temp\_}\hat{D}_x^n + A_{4z}\Delta t\phi_x^{n+1}.$$

7th step:

$$D_x^{n+1} = e^{-A_{1z}\Delta t}\text{temp\_}D_x^n + \hat{D}_x^{n+1} - e^{-A_{1z}\Delta t}\text{temp\_}\hat{D}_x^n + A_{3z}\Delta t\phi_x^{n+1}.$$

Similar operations can be applied to 2nd-order DZT-CFS-UPML.

III. Numerical Results

To reflect preferable performances between the proposed 1st- and 2nd-order DZT-CFS-UPML approaches for relevant FDTD cases so that we can judge which one is the best choice for the corresponding FDTD case, we get ready to adopt commonly used 2-D and 3-D cases for assessing their comprehensive performances.

In the first case, a 2-D TE-polarized electromagnetic wave interaction with an infinitely long perfectly electric conductor (PEC) sheet with the finite width is applied to illustrating the validity of the proposed DZT-CFS-UPMLs.

The space is discretized with $\Delta x = \Delta y = 1$ mm and time step is $\Delta t = 1.1785$ ps. The FDTD computational domain consists of a 100-cell wide PEC sheet surrounded by free space. The ten cell-thick PML layers are used to terminate the grid and are placed only three cells away from the PEC sheet in all directions, shown in Fig. 1.

A y-polarized line electric current source, infinitely long in the z-direction, is placed at the center position and excited with the differentiated Gaussian pulse [26]. The y-component of the electric field is measured at the observing point P, where we expect very strong evanescent waves to appear.

The relative reflection error (in dB) versus time steps is computed at the observation point P. The reference grid is sufficiently large such that there are no reflections from its outer boundaries during 1500 time steps, which are well past the steady-state response.

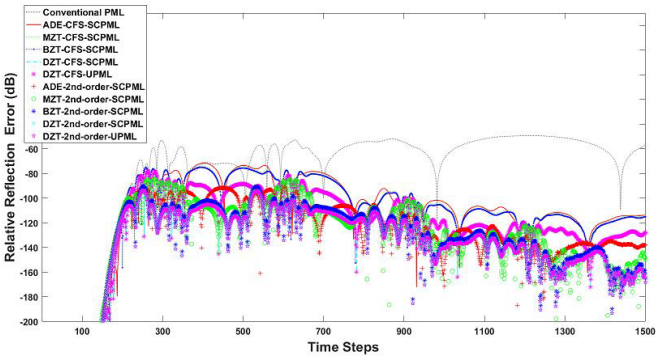

Fig. 2. Relative reflection error versus time steps.

TABLE I
Performances for Different PML Implementations

PML algorithms	MRRE (dB)	Memory (bytes)	CPU time (s)
Conventional PML	-49.1982	1,324 K	66.79
ADE-CFS-SCPML	-71.4797	1,161 K	66.51
MZT-CFS-SCPML	-73.6765	1,176 K	66.75
BZT-CFS-SCPML	-74.9075	1,172 K	67.25
DZT-CFS-SCPML	-77.2969	1,281 K	74.95
DZT-CFS-UPML	-77.7969	1,403 K	80.65
ADE-2nd-order-SCPML	-90.4784	1,375 K	88.95
MZT-2nd-order-SCPML	-84.3734	1,353 K	88,65
BZT-2nd-order-SCPML	-90.2828	1,353 K	88.95
DZT-2nd-order-SCPML	-93.7828	1,457 K	88.95
DZT-2nd-order-UPML	-93.7828	1,711 K	89.95

The details of PML parameters have been presented to obtain the lowest reflection, shown as follows.

1) For the conventional PML, $\kappa_{\max} = 9$ and $\sigma_{\max} = 0.6\sigma_{\text{opt}}$ are chosen.
2) For the CFS-PML,$\kappa_{\max} = 9$, $\sigma_{\max} = 0.9\sigma_{\text{opt}}$, and $\alpha_\eta = 0.05$ are chosen.
3) For the 2nd-order PML, the following parameters are chosen:

$$\kappa_{1\eta} = 1, \alpha_{1\eta} = 0, \sigma_{1\eta\text{opt}} = 0.075/150\pi\,\Delta x, \sigma_{1\eta} = \sigma_{1\eta\text{opt}}\rho^4$$
$$\sigma_{2\eta\text{opt}} = 4/150\pi\,\Delta x, \sigma_{2\eta} = \sigma_{2\eta\text{opt}}\rho^2, \kappa_{2\eta} = 1 + \kappa_{2\eta\text{opt}}\rho^2,$$
$$\kappa_{2\eta\text{opt}} = 10, \text{and}\alpha_{2\eta} = 0.08 + \sigma_{1\eta}.$$

These optimum parameters are empirically chosen to reach the lowest reflection.

The results are illustrated in Fig. 2. The maximum relative reflection errors (MRRE), memory requirements, and CPU time consumption (time steps = 20 000) for these PMLs are shown in Table I.

As it is reflected in Fig. 2 and Table I that the case has been used to validate all FDTD methods with PML scheme. In Fig. 2, the proposed 1st-order DZT-CFS-UPML has similar accuracy with the 1st-order DZT-CFS-SCPML.

However, for this 2-D case, we can see in Fig. 2 that the 2nd-order one has more obvious improvement than the

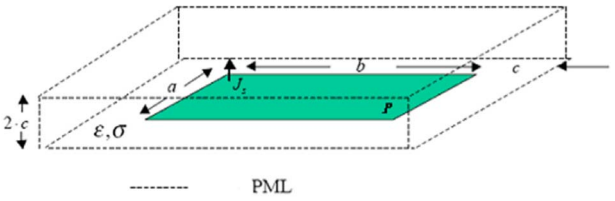

Fig. 3. FDTD grid geometry in this simulation.

1st-order one, although a bit more time and memory are required, shown in Table I. Therefore, the 2nd-order DZT-CFS-UPML can be considered as the preferable choice when solving 2-D FDTD problems.

It should be noted in the first case, however, that the advantages of the 1st-order DZT-CFS-UPML is not quite obvious due to only solving the 2-D case. To better reflect its advantages, therefore, the 3-D problem of the electromagnetic scattering by a highly elongated object is studied [29].

The thin plate with the 100 mm $\times$25 mm size is immersed in a background media [29] with constitutive parameters σ and ε, shown in Fig. 3. For the purpose of this study, the constitutive parameters for soil are assumed, using $\varepsilon_r = 7.73$ and $\sigma = 0.273$. The numerical test is implemented and composed of a 126 $\times$51 $\times$26 grid, which includes ten cell-thick PML. The space is discretized with the FDTD lattice with $\Delta x = \Delta y = \Delta z = 1$ mm and the time step is $\Delta t = 5.3$ ps. In total, 2000 time steps are used for computing the relative reflection error versus time at an observation point. All similar details of this numerical simulation can be found in [29].

The details of PML parameters have been presented to obtain the lowest reflection, shown as follows.

1) For the conventional PML, $\kappa_{\max} = 14$ and $\sigma_{\max} = 0.56\sigma_{\text{opt}}$ are chosen.
2) For the CFS-PML,$\kappa_{\max} = 11$, $\sigma_{\max} = 0.4\sigma_{\text{opt}}$, and $\alpha_\eta = 0.05$ are chosen.
3) For the 2nd-order PML, the following parameters are chosen:

$$\kappa_{1\eta} = 1, \alpha_{1\eta} = 0, \sigma_{1\eta\text{opt}} = 0.075/150\pi\,\Delta x, \sigma_{1\eta} = \sigma_{1\eta\text{opt}}\rho^4,$$
$$\sigma_{2\eta} = \sigma_{2\eta\text{opt}}\rho^2, \kappa_{2\eta} = 1 + \kappa_{2\eta\text{opt}}\rho^2, \kappa_{2\eta\text{opt}} = 14,$$
$$\alpha_{2\eta} = 0.06 + \sigma_{1\eta}, \text{and } \sigma_{2\eta\text{opt}} = 4/150\pi\,\Delta x.$$

These optimum parameters are empirically chosen to reach the lowest reflection.

As seen in Fig. 4 and Table II, it can be observed that the 1st- and 2nd DZT-based SC and UPMLs have better absorption with the increasing of time steps and much more reduction in the late-time reflection than the other PMLs based on ADE, BZT, and MZT.

Furthermore, as presented in Table II, the 1st-order DZT-CFS-UPML not only requires much less CPU time and memory than the 2nd-order DZT-CFS-UPML but also obtains very good absorption accuracy, although higher absorption accuracy can be reached using the 2nd-order one. Therefore, the 1st-order DZT-CFS-UPML can be treated as the preferable choice when solving 3-D FDTD problems.

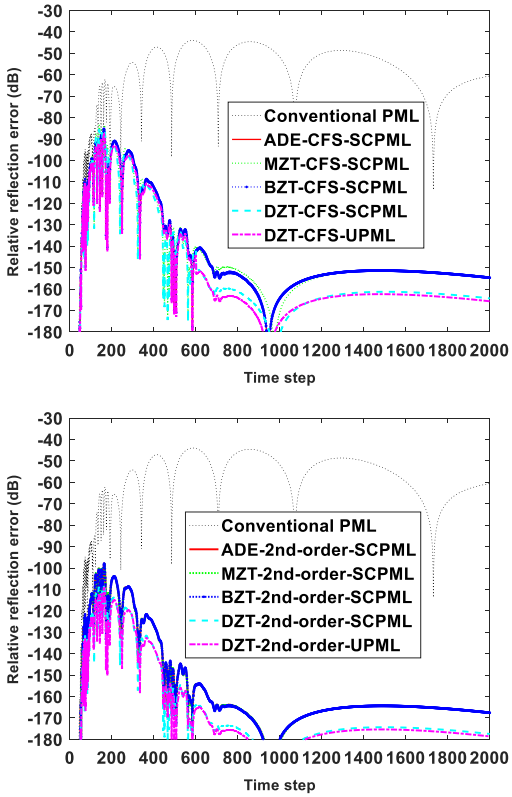

Fig. 4. Relative reflection errors versus time steps for the 1st- and 2nd-order DZT-CFS-UPMLs.

TABLE II
PERFORMANCES FOR DIFFERENT PML IMPLEMENTATIONS

PML algorithms	MRRE (dB)	Memory (bytes)	CPU time (s)
Conventional PML	-43.9754	26,334 K	780.79
ADE-CFS-SCPML	-85.2538	25,361 K	777.51
MZT-CFS-SCPML	-83.5343	25,276 K	776.75
BZT-CFS-SCPML	-85.2538	25,372 K	777.25
DZT-CFS-SCPML	-85.5343	26,121 K	776.95
DZT-CFS-UPML	-87.2538	28,503 K	798.65
ADE-2nd-order-SCPML	-97.7774	31,275 K	1031.08
MZT-2nd-order-SCPML	-97.5969	31,335 K	1033.12
BZT-2nd-order-SCPML	-97.9582	31,311 K	1031.03
DZT-2nd-order-SCPML	-107.4053	32,551 K	1061.52
DZT-2nd-order-UPML	-109.0646	33,221 K	1082.81

IV. CONCLUSION

So far, the validities and stabilities of the proposed 1st- and 2nd-order DZT-CFS-UPMLs have been illustrated. Additionally, for the relevant FDTD cases, we can judge and determine which one is the best choice between 1st- and 2nd-order DZT-CFS-UPMLs, in terms of the tradeoff among CPU time, memory requirement, and absorption accuracy. In a word, due to introducing the DZT techniques, the proposed 1st- and 2nd-order CFS-UPMLs can not only achieve better accuracies than those based on ADE, BZT, and MZT but also provide alternative choices of DZT-based UPML implementations and make themselves easily mastered and used.

REFERENCES

[1] J. A. Roden and S. D. Gedney, "Convolution PML (CPML): An efficient FDTD implementation of the CFS-PML for arbitrary media," *Microw. Opt. Technol. Lett.*, vol. 27, no. 5, pp. 334–339, Dec. 2000.

[2] O. Ramadan, "Auxiliary differential equation formulation: An efficient implementation of the perfectly matched layer," *IEEE Microw. Wireless Compon. Lett.*, vol. 13, no. 2, pp. 69–71, Feb. 2003.
[3] J. Li and J. Dai, "An efficient implementation of the stretched coordinate perfectly matched layer," *IEEE Microw. Wireless Compon. Lett.*, vol. 17, no. 5, pp. 322–324, May 2007.
[4] O. Ramadan and A. Y. Oztoprak, "DSP techniques for implementation of perfectly matched layer for truncating FDTD domains," *Electron. Lett.*, vol. 38, no. 5, pp. 211–212, Feb. 2002.
[5] D. M. Sullivan, "Frequency-dependent FDTD methods using Z transforms," *IEEE Trans. Antennas Propag.*, vol. 40, no. 10, pp. 1223–1230, Oct. 1992.
[6] J. Li and J. Dai, "Efficient implementation of stretched co-ordinate perfectly matched layer using DSP techniques," *Electron. Lett.*, vol. 42, no. 17, pp. 953–955, 2006.
[7] J. Li and J. Dai, "Efficient implementation of the stretched co-ordinate perfectly matched layer based on the Z-transform method," *IET Microw. Antennas Propag.*, vol. 1, no. 3, pp. 645–650, 2007.
[8] O. Ramadan and A. Y. Oztoprak, "Z-transform implementation of the perfectly matched layer for truncating FDTD domains," *IEEE Microw. Wireless Compon. Lett.*, vol. 13, no. 9, pp. 402–404, Sep. 2003.
[9] G.-X. Fan and Q. H. Liu, "An FDTD algorithm with perfectly matched layers for general dispersive media," *IEEE Trans. Antennas Propag.*, vol. 48, no. 5, pp. 637–646, May 2000.
[10] S. D. Gedney, "An anisotropic PML absorbing media for the FDTD simulation of fields in lossy and dispersive mediaz," *Electromagnetics*, vol. 16, no. 4, pp. 399–415, 1996.
[11] S. D. Gedney, "An anisotropic perfectly matched layer-absorbing medium for the truncation of FDTD lattices," *IEEE Trans. Antennas Propag.*, vol. 44, no. 12, pp. 1630–1639, Dec. 1996.
[12] J.-P. Berenger, "A perfectly matched layer for the absorption of electromagnetic waves," *J. Comput. Phys.*, vol. 114, no. 2, pp. 185–200, 1994.
[13] K. S. Yee, "Numerical solution of initial boundary value problems involving Maxwell's equations in isotropic media," *IEEE Trans. Antennas Propag.*, vol. AP-14, no. 3, pp. 302–307, Mar. 1966.
[14] D. M. Sullivan, *Electromagnetic Simulation Using the FDTD Method*. New York, NY, USA: Wiley, 2000.
[15] J. G. Proakis and D. G. Manolakis, *Digital Signal Processing: Principles, Algorithms, and Applications*, 3rd ed. Upper Saddle River, NJ, USA: Prentice-Hall, 1996.
[16] M. Kuzuoglu and R. Mittra, "Frequency dependence of the constitutive parameters of causal perfectly matched anisotropic absorbers," *IEEE Microw. Guided Wave Lett.*, vol. 6, no. 12, pp. 447–449, Dec. 1996.
[17] J. Li and J. Dai, "Z-transform implementation of the CFS-PML for arbitrary media," *IEEE Microw. Wireless Compon. Lett.*, vol. 16, no. 8, pp. 437–439, Aug. 2006.
[18] D. Correia and J.-M. Jin, "A simple and efficient implementation of CFS-PML in the FDTD analysis of periodic structures," *IEEE Microw. Wireless Compon. Lett.*, vol. 15, no. 7, pp. 487–489, Jul. 2005.
[19] J. Li and J. Dai, "Z-transform implementations of the CFS-PML," *IEEE Antennas Wireless Propag. Lett.*, vol. 5, no. 1, pp. 410–413, Dec. 2006.
[20] N. Feng, Y. Yue, C. Zhu, Q. H. Liu, and L. Wan, "Efficient Z-transform implementation of the D-B CFS-PML for truncating multiterm dispersive FDTD domains," *Appl. Comput. Electromagn. Soc. J.*, vol. 29, no. 3, pp. 190–196, Mar. 2014.
[21] X. Zhuansun and X. Ma, "Integral-based exponential time differencing algorithms for general dispersive media and the CFS-PML," *IEEE Trans. Antennas Propag.*, vol. 60, no. 7, pp. 3257–3264, Jul. 2012.
[22] D. Correia and J.-M. Jin, "On the development of a higher-order PML," *IEEE Trans. Antennas Propag.*, vol. 53, no. 12, pp. 4157–4163, Dec. 2005.
[23] N. Feng and J. Li, "Efficient DSP-higher-order PML formulations for the metal plate buried in dispersive soil half-space problem," *IEEE Trans. Electromagn. Compat.*, vol. 54, no. 5, pp. 1178–1181, Oct. 2012.
[24] N. Feng and Q. H. Liu, "Efficient implementation of multi-pole UPML using trapezoidal approximation for general media," *J. Appl. Geophys.*, vol. 111, pp. 59–65, Dec. 2014.
[25] A. Giannopoulos, "Unsplit implementation of higher order PMLs," *IEEE Trans. Antennas Propag.*, vol. 60, no. 3, pp. 1479–1485, Mar. 2012.
[26] N. Feng and J. Li, "Novel and efficient FDTD implementation of higher-order perfectly matched layer based on ADE method," *J. Comput. Phys.*, vol. 232, no. 1, pp. 318–326, Jan. 2013.
[27] N.-X. Feng, J.-X. Li, and X.-M. Zhao, "Efficient FDTD implementations of the higher-order PML using DSP techniques for arbitrary media," *IEEE Trans. Antennas Propag.*, vol. 61, no. 5, pp. 2623–2629, May 2013.
[28] N. Feng, Y. Yue, C. Zhu, L. Wan, and Q. H. Liu, "Second-order PML: Optimal choice of nth-order PML for truncating FDTD domains," *J. Comput. Phys.*, vol. 285, pp. 71–83, Mar. 2015.
[29] N. Feng, Y. Yue, and Q. H. Liu, "Direct Z-transform implementation of the CFS-PML based on memory-minimized method," *IEEE Trans. Microw. Theory Tech.*, vol. 63, no. 3, pp. 877–882, Mar. 2015.

Naixing Feng (S'16–M'18) received the B.S. degree in electronic science and technology and the M.S. degree in micro-electronics and solid-state electronics from Tianjin Polytechnic University, Tianjin, China, in 2010 and 2013, respectively, and the Ph.D. degree from the College of Electronic Science and Technology, Xiamen University, Xiamen, China, in 2018.

He has studied and worked as a Visiting Scholar supported by the CSC at the Department of Electrical and Computation Engineering, Duke University, Durham, NC, USA, from 2015 to 2016. He is currently an Associate Professor with the Institute of Microscale Optoelectronics, Shenzhen University, Shenzhen, China. He has authored or coauthored around 40 papers published by refereed international journals and conference and is the holder of one patent. His current research interests are mainly in the areas of computational electromagnetics and acoustics, geophysics, and nanophotonics and 2D materials and their applications.

Jingang Wang received the Ph.D. degree from the College of Chemistry, Liaoning University, Shenyang, China, in 2018.

From 2015 to 2018, he was studying at the Beijing National Laboratory for Condensed Matter Physics, Institute of Physics, Chinese Academy of Sciences (CAS), Beijing, China. In 2018, he was an Associate Professor with the College of Science, Liaoning Shihua University, Fushun, China. He is currently focusing on the properties and application of two dimensional (2D) materials, plasmonics, and nonlinear optics.

Jinfeng Zhu (M'15–SM'17) received the B.S. degree in electronic communication science and technology and the Ph.D. degree in physical electronics from the University of Electronic Science and Technology of China, Chengdu, China, in 2006 and 2012, respectively.

From November 2009 to November 2011, he was a Visiting Researcher with the Device Research Lab and the Department of Electrical Engineering, University of California, Los Angeles, CA, USA, under the financial support from the China Scholarship Council. Since July 2012, he has been with Xiamen University, Xiamen, Fujian, China, where he is currently an Associate Professor of electrical engineering. He has authored and coauthored over 40 peer-reviewed journals and conference papers. His research interests include nanoantennas, nanophotonics, plasmonics, metamaterials, and van der Waals materials.

Dr. Zhu is a member of the Optical Society of America, and has served as a reviewer for many academic journals, including *ACS Nano*, *Nanoscale*, *ACS Photonics*, *Optics Express*, and the IEEE PHOTONICS JOURNAL.

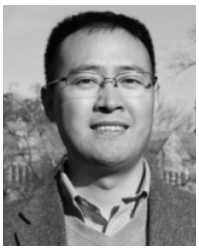

Zhongzhu Liang received the B.S. degree from the College of Materials Science and Engineering, Jilin University, Changchun, China, in 2002, and the Ph.D. degree from the State Key Laboratory of Superhard Materials, Jilin University, in 2007, majoring in the synthesis and optical characterization of the diamond with nitrogen impurities.

From December 2013 to January 2015, he was a Visiting Scholar with the Electrical and Computer Engineering, Duke University, Durham, NC, USA, under the financial support from the China Scholarship Council. He was appointed as a Professor with the State Key Laboratory of Applied Optics, Changchun Institute of Optics, Fine Mechanics and Physics, Chinese Academy of Sciences, Beijing, China, in September 2014. He has authored and coauthored more than 90 peer-reviewed journals and conference papers. His research interests include micro-optical electro-mechanical-system, plasmonics, and sensors.

Guo Ping Wang received the Ph.D. degree from Sichuan University, Chengdu, China.

He furthered his research as a Post-Doctoral Fellow at Osaka University, Suita, Japan, and also a Visiting Scholar at the Tokyo Institute of Technology, Tokyo, Japan, The Hong Kong University of Science and Technology, Hong Kong, and Nanyang Technological University, Singapore. After that, he worked at Wuhan University, Wuhan, China, as the second rank Professor and the Distinguished Professor with Luojia Scholar. He is currently a Distinguished Professor with Shenzhen University, Shenzhen, China, honored as the National Leading Talents in Shenzhen. He obtained several innovative achievements in the research of optical metamaterials, optical super-resolution imaging and sensors, optical cloaking, nanophotonics, and other frontiers, and has published more than 90 pre-reviewed journal articles with more than 50 articles being published on *Nature Communications*, *Physical Review Letters*, *Physical Review B (Rapid Communications)*, *Applied Physics Letters*, *Optics Letters*, *Optics Express*, *Nanoscale*, and *Scientific Reports*. In addition, he contributed more than 20 invited talks in international conferences and has coauthored the book named *Plasmonic Nanoguides and Circuits*.

Dr. Wang received the National Natural Science Foundation of China for Distinguished Young Scholars, the State Council Special Allowance, and supported by the Program for New Century Excellent Talents in the University of Ministry of Education of China. For the excellent work, he was a recipient of numerous awards, including the second class of the State Natural Science Award, the first class of the Hubei Natural Science Award, the first class of Hubei Education Achievements Award, and the first session of the Excellent University Key Teacher Award of the Ministry of Education of China. Meanwhile, he is a fellow of the Information Science Department and the Mathematical and Physical Science Department of the National Natural Science Foundation of China, and presides over 20 projects, including the National Science Foundation of China for Distinguished Young Scientists, the National Basic Research Program of China (973 Program), the Key Program of the National Natural Science Foundation of China, and the Program for New Century Excellent Talents in University of Ministry of Education of China.

William T. Joines (M'61–SM'94–LSM'97–LF'08) was born in Granite Falls, NC, USA. He received the B.S.E.E. degree (Hons.) from North Carolina State University, Raleigh, NC, USA, in 1959, and the M.S. and Ph.D. degrees in electrical engineering from Duke University, Durham, NC, USA, in 1961 and 1964, respectively.

From 1959 to 1966, he was a member of the Technical Staff with Bell Telephone Laboratories, where he was involved in research and development of microwave components and systems for military applications. He also served as a Radar Technician for the U.S. Air Force. He is currently a Professor in the Sensing and Signals Group with the Department of Electrical and Computer Engineering, Duke University, where his research and teaching focuses on electromagnetic field and wave interactions with materials and structures, especially in the microwave and optical frequency ranges where wavelengths are commensurate with important structures (antennas, circuit elements, and the human body). He has supervised more than 60 graduate students in their thesis and dissertation research, leading to their M.S. and Ph.D. degrees. He has authored or coauthored over 300 technical papers on electromagnetic wave theory and applications, and holds 21 U.S. patents.

Dr. Joines was a recent recipient of the Outstanding Engineering Educator Award from the IEEE, and the Scientific and Technical Achievement Award presented by the Environmental Protection Agency in 1982, 1985, and 1990.